Version 00 as of November 13, 2019
Primary authors: Carlos Yero, Werner Boeglin, Mark Jones
To be submitted to PRL
Comment to cyero002@fiu.edu by xxx, yyy

DØ INTERNAL DOCUMENT – NOT FOR PUBLIC DISTRIBUTION

First Measurements of the D(e,e'p)n Cross Section at Very High Recoil Momenta and Large Q^2

C. Yero and W.U. Boeglin
Florida International University, University Park, Florida 33199, USA

M.K. Jones
Thomas Jefferson National Accelerator Facility, Newport News, Virginia 23606, USA

(for the Hall C Collaboration)

(Dated: November 13, 2019)

First results of cross section measurements of the $^2H(e,e'p)n$ reaction at 4-momentum transfers $4 \leq Q^2 \leq 5$ GeV^2 and neutron recoil momenta up to $p_r \sim$1.18 GeV/c are presented. At the selected kinematics, Meson Exchange Currents (MEC) and Isobar Configurations (IC) are suppressed. Final State Interactions (FSI) have also been suppressed by choosing a kinematic region where the in-plane neutron recoil angle (θ_{nq}) is between 35 and 45 degrees with respect to the 3-momentum transfer, $\vec{q}$. In this region, the Plane Wave Impulse Approximation (PWIA) dominates and comparison to recent theoretical calculations show data to be sensitive to momentum distributions up to $p_r \sim 700$ MeV/c.

Being the only bound two-nucleon system, the deuteron serves as a starting point to study the strong nuclear force at the subfermi level which is currently not well understood. At such small internucleon distances the NN (nucleon-nucleon) potential is expected to exhibit a repulsive core in which the interacting nucleon pair begins to overlap. The overlap is directly related to two-nucleon short range correlations (SRC) observed in $A > 2$ nuclei [1–4]. Short-range studies of the deuteron are also important in determining whether or to what extent is the description of nuclei in terms of nucleon/meson degrees of freedom valid before having to include explicit quark effects, which is an issue of fundamental importance in nuclear physics[5]. As of the present time, there are only a few nuclear physics experiments for which a transition between nucleonic to quark degrees of freedom been observed [6–8]. This Letter presents first results of $^2H(e,e'p)n$ in which kinematics were taken to the limit where a transition to non-nucleonic degrees of freedom is expected.

The most direct way to study the short range structure of the deuteron wavefunction (or equivalently, its high momentum components) is via the exclusive deuteron electro-disintegration reaction at very high neutron recoil (or missing) momenta and within the PWIA kinematics. In this approximation, the virtual photon couples to the proton which is ejected from the nucleus without further interaction with the recoiling neutron, which carries a momentum equal in magnitude but opposite in direction to the initial state proton, $\vec{p}_r = -\vec{p}_{i,p}$. This gives direct access to the deuteron momentum distributions since the scattered neutron momentum remains unchanged from its initial state.

In reality, the ejected particles undergo subsequent interactions resulting in re-scattering between the proton and neutron (FSIs). Another possibility is that the photon may couple to the virtual meson being exchanged between the nucleons (MECs), or the photon may excite either nucleon in the deuteron into a resonance state (ICs) which decays back into the ground state nucleon causing futher re-scattering between the proton and neutron. Both MECs and ICs in addition to FSIs can significantly alter the recoiling neutron momentum thereby obscuring any possibility of directly accessing the deuteron momentum distributions.

Previous deuteron electro-disintegration experiments performed at Jefferson Lab (JLab) have helped constrain and quantify the contributions from FSIs, MECs and ICs on the $^2H(e,e'p)n$ cross-section and determine the kinematics at which they are either suppressed (MECs and ICs) or under control (FSIs). The first of these was performed in Hall A [9] at a relatively low momentum transfer of $Q^2 = 0.665$ GeV^2 and neutron recoil momenta up to $p_r = 550$ MeV/c where it was shown that for $p_r > 300$ MeV/c, FSIs, MECs and ICs played a significant role and their inclusion was necessary in Arenhövel's calculations [10–13] for a satisfactory agreement between theory and data.

The next experiment was performed in Hall B [14] using the CEBAF Large Acceptance Spectrometer (CLAS) which measured a wide variety of kinematic settings giving an overview of the $^2H(e,e'p)n$ reaction kinematics.

This was the first experiment to probe the deuteron at high momentum transfers ($1.75 \leq Q^2 \leq 5.5$ GeV^2) and presented angular distributions of cross-sections that confirmed the onset of the General Eikonal Approximation (GEA)[15, 16], which predicts a strong angular dependence of FSI with neutron recoil angles with a peak at $\theta_{nq} \sim 70^o$. The cross sections versus neutron recoil momenta up to $p_r \sim$2 GeV/c were also presented, however, due to statistical limitations it was impossible to select kinematical bins in θ_{nq} where FSIs were small to extract momentum distributions.

Finally, a third $^2H(e,e'p)n$ experiment was performed in Hall A [17] at published $Q^2 = 3.5 \pm 0.25$ GeV^2 and recoil momenta up to 550 MeV/c. The angular distributions of the cross-section ratio ($R = \sigma_{exp}/\sigma_{PWIA}$) versus θ_{nq} presented verified the strong anisotropy of FSIs with recoil angle also observed in Hall B[14]. Most importantly, for recoil neutron momentum bins, $p_r = 0.4 \pm 0.02$ and 0.5 ± 0.02 GeV/c, the ratio was found to be $R \sim 1$ for $35^o \leq \theta_{nq} \leq 45^o$ indicating a reduced sensitivity of the experimental cross-section to FSIs. This kinematic window allowed for the first time the extraction of momentum distributions for neutron recoil momenta up to $p_r \sim$550 MeV/c.

The experiment presented on this Letter takes advantage of the kinematic window previosuly found in Hall A[17] and extends the $^2H(e,e'p)n$ cross section measruements to $Q^2 = 4.5 \pm 0.5$ GeV^2 and neutron recoil momenta up to 1.18 GeV/c. At these kinematics, MECs and ICs are suppressed and FSIs are under control for neutron recoil angles between 35 and 45 degrees giving access to unprecedented high momentum components of the deuteron wavefunction.

This experiment was part of a group of four experiments that commissioned the new Hall C Super High Momentum Spectrometer (SHMS) as part of the 12 GeV upgrade at JLab. A 10.6005 GeV electron beam was incident on a 10 cm long liquid deuterium target (LD2). The scattered electron and knocked-out proton were detected in coincidence by the SHMS and High Momentum Spectrometer (HMS), respectivly. The "missing" (undetected) neutron was reconstructed from momentum conservation laws. The beam currents delivered by the accelerator ranged between 40-60 μA due to frequent beam trips at higher currents and the beam was rastered over a 2x2 mm^2 area to reduce the effects of localized boiling on the cryogenic targets (hydrogen and deuterium).

Both spectrometers at Hall C have similar standard detector packages, each with 1) four sets of hodoscope planes[18] (scintillator arrays) used for triggering, 2) a pair of drift chambers[19] used for tracking, 3) a calorimeter[20] used for e^-/π^- discrimination and 4) a gas Čerenkov [21, 22] used also for e^-/π^- separation. Due to the absence of significant background on this experiment and the low coincidence trigger rates ($\sim 1-3$ Hz) at the higher missing momentum settings, the use of additional particle identification (PID) was found to have little to no effect on the final cross section.

We measured three missing momentum settings: $p_r = 80, 580$ and 750 MeV/c. In the high missing momentum settings the spectrometer configuration was changed multiple times resulting in either the spectrometer angle or momentum not being exactly the same. As a result, two separate data sets were measured for the 580 MeV/c setting and three data sets for the 750 MeV/c setting. The spectrometer central settings are approximately as follows: the SHMS central angle and momentum settings were kept "fixed" at ($\sim$12.194 deg, 8.5342 GeV/c) and the HMS central angle and momentum settings were changed from (38.896 deg, 2.840 GeV/c) at the 80 MeV setting to $\sim$(54.992 deg, 2.1925 GeV/c) and $\sim$(58.391 deg, 2.0915 GeV/c) at the 580 and 750 MeV/c settings, respectively.

At these kinematics, the 3-momentum transfer is $|\vec{q}| \sim$ 2.88 GeV/c which is more than twice the highest neutron recoil momentum (p_r) measured on this experiment. As a result one can infer that most of the virtual photon momentum is transferred to the proton. This configuration is known as the "parallel-kinematics" and suppresses the process in which the neutron is struck while the detected proton is a spectator. FSIs are also expected to be largely reduced as compared to the "perpendicular-kinematics" in which the proton is detected almost perpendicular to $\vec{q}$ based on a calculation by Arenhövel on Table 1 of Ref.[5].

In addition to deuteron kinematics, $^1H(e,e'p)$ elastic data was also taken at kinematics close to the deuteron 80 MeV setting for cross-checks with the spectrometer acceptance model as well as for normalization purposes using the Hall C Monte Carlo simulation program, SIMC. Additional $^1H(e,e'p)$ data was also taken at three other kinematic settings that covered the entire SHMS momentum acceptance range and were used for spectrometer optics optimization, momentum calibration and determination of the spectrometer offsets and kinematic uncertainties[23, 24].

The event selection criteria was done exactly the same for the hydrogen and deuteron data. The criteria was determined by making 1) standard cuts on the spectrometer momentum fraction (δ) to select a region in which the reconstruction optics is well known, 2) an HMS collimator cut to restrict the spectrometer solid angle acceptance to events that only passed through the collimator and not by re-scattering from the collimator edges, 3) a missing energy cut (peak $\sim$ 2.22 MeV for the deuteron) to select true ep coincidences and not events from the radiative tail, 4) a coincidence time cut to select true coincidence events and not accidentals, 5) a PID cut on the SHMS calorimeter to select electrons and not other sources of background, mostly pions and 6) a z-vertex difference cut between the HMS and SHMS z reaction vertex difference to select events that truly originated from the same reaction vertex at the target.

The experimental data yield was normalized by the total charge and corrected for tracking efficiencies, total live time, proton absorption[25] and target boiling factors[26]. For $^1H(e,e'p)$, the corrected data yield was compared to SIMC using P. Bosted's proton form factor parametrization[27] to check the spectrometer acceptance model. The data to SIMC yield ratio integrated over invariant mass W was determined to be unity, so there was no need to include an overall hydrogen normalization factor. For the $^2H(e,e'p)n$ data, the measured cross sections were compared to the model cross sections (incorporated as a SIMC subroutine) from calculations by J.M. Laget using the Paris potential. Variations of up to $\sim$ 20% for recoil momenta up to $\sim$ 250 MeV/c were observed which are typical for this setting using the Paris potential. The 80 MeV data was also checked for reproducibility against the Hall A data (See Fig. 2). This agreement gives us confidence on the measurements made at higher missing momentum setting for which no data exists.

The systematic uncertainties on the measured cross sections were determined from normalization[28] and kinematic uncertainties. The individual contributions from normalization uncertainties were determined to be: tracking efficiencies (0.40%-HMS, 0.59%-SHMS), target boiling (0.39%), total live time (3.0%) and total charge (2.0%) for an overall normalization uncertainty added in quadrature of 3.7%.

The kinematic uncertainties were determined point-to-point in (θ_{nq}, p_r) bins for each data set independently, and added in quadrature for overlapping p_r bins of different data sets. For $\theta_{nq} = 35$, 45 and 75 deg (presented on this Letter) the overall kinematic uncertainty varied up to 6.5% for $p_r \leq 1.01$ GeV/c. The overall systematic uncertainty in the cross section was determined by the quadrature sum of the normalization and kinematic uncertainties. This results was then added in quadrature to the statiscial uncertainty to obtain the final uncertainty in the cross section.

The data was radiatively corrected for each bin in (θ_{nq}, p_r) by multiplying measured cross sections to the ratio of the SIMC yield without and with radiative effects. Bin-centering corrections were also applied by multiplying the radiative corrected cross sections to the ratio of theoretical cross sections (external to SIMC) to the average cross sections calculated from SIMC. The theoretical calculations used in the bin-centering corrections were done by J.M. Laget using the Paris potential[29].

Both experimental and theoretical reduced cross sections were extracted from the measured (or model) cross sections for each data set independently and were averaged for overlapping bins in p_r, where the reduced cross sections are defined as follows:

$$\sigma_{red} \equiv \frac{\sigma_{exp(th)}}{K f_{rec} \sigma_{cc1}} \qquad (1)$$

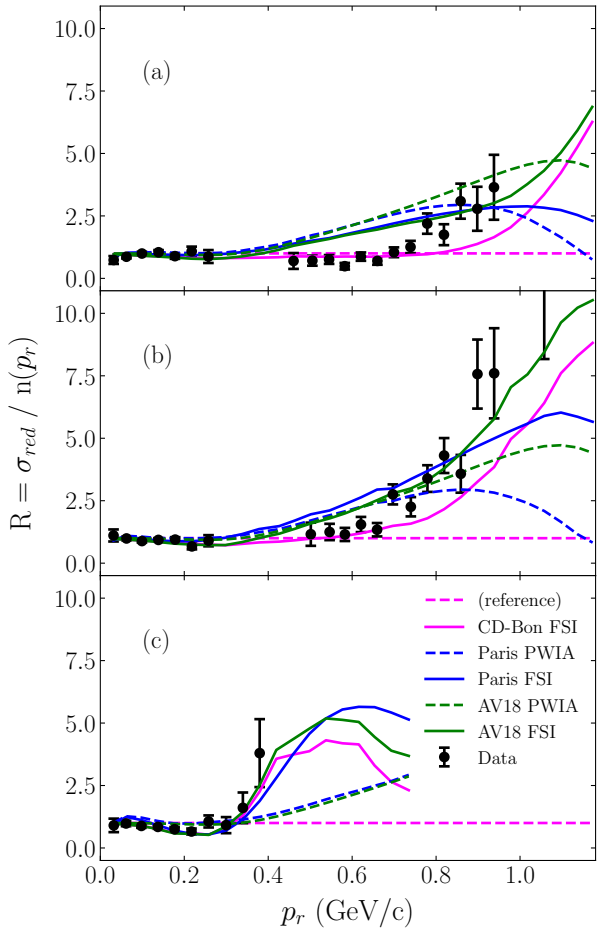

FIG. 1. The ratio $R(p_r) = \sigma_{red}/n(p_r)$ is shown in (a)-(c) for $\theta_{nq} = 35^o, 45^o$ and 75^o, respectively, each with a bin width of $\pm 5^o$. The dashed reference (magenta) line refers to CD-Bonn momentum distribution ($n(p_r)$) by which the data and all models are divided.

where $\sigma_{exp(th)}$ is the 5-fold experimental (or theoretical) differential cross section $\frac{d^5\sigma}{d\omega d\Omega_e d\Omega_p}$, K is a kinematical factor, f_{rec} is a the recoil factor that arises from the integration over missing energy and σ_{cc1} is the de Forest[30] electron-proton offshell cross section calculated using P. Bosted's form factor parametrization [27]. Only within the PWIA, can σ_{red} be interpreted as the proton momentum distribution inside the deuteron where most of the kinematical dependencies that arise from the cross section have been factored out by σ_{cc1}, leaving only a dependency on p_r.

To quantify by how much and to what extent the data agrees with theory, the ratio of the experimental (or theoretical) reduced cross sections (σ_{red}) relative to the deuteron momentum distributions ($n(p_r)$) using the charge-dependent Bonn (CD-Bonn) potential[31] is shown in Fig. 1. The theoretical calculations for the CD-Bonn and Argonne v_{18}[32] (AV18) potentials were

performed by M. Sargsian and those for the Paris potential were done by J.M. Laget. For $p_r \lesssim 300$ MeV/c, the data is in good agreement with all models for the neutron recoil angles shown in Fig. 1. For $p_r \gtrsim 300$, at recoil angles $\theta_{nq} = 35^o \pm 5^o$ [Fig. 1(a)], the data is best described by the CD-Bonn curves which exhibit a reduced sensitivity to FSIs and an enhanced sensitivity to the momentum distribution with a ratio R∼1 for recoil momenta up to ∼ 800 MeV/c before being overwhelmed by FSIs. The data, however, is sensitive to the momentum distributions only up to $p_r \sim 750$ MeV/c before transitioning to other theoretical curves with a maximal ratio of R∼3 at p_r ∼940 MeV/c due to statistical limitations. For recoil angles $\theta_{nq} = 45^o \pm 5^o$ [Fig. 1(b)], both the data and CD-Bonn curves show sensitivities to momentum distributions up to $p_r \sim 580$ MeV/c. At $p_r > 580$ MeV/c, FSIs become increasingly important for CD-Bonn, whereas the data shows a similar behaviour as in Fig. 1(a) with an early rise in the ratio than predicted by the CD-Bonn FSI model. For $\theta_{nq} = 75^o \pm 5^o$ [Fig. 1(c)], the onset of GEA is observed beyond $p_r \sim 300$ MeV/c, with a strong angular dependence of the reduced cross sections on FSIs predicted by all models and verified by data which was statistically limited at larger recoil angles.

Figure 2 shows the extracted experimental and theoretical reduced cross sections as a function of neutron recoil momentum, p_r for three angular settings at $4 \leq Q^2 \leq 5$ $(\mathrm{GeV/c})^2$. The data is compared to the results from the previous Hall A experiment[17] at a $Q^2 = 3.5$ $(\mathrm{GeV/c})^2$. The overlay of the Hall A data (cyan) in Fig. 2 provides a continutity to the data from this experiment in the transition from low (80 MeV/c) to high (580, 750) MeV/c missing momentum settings in which there was no data. There is also an overall good agreement between the two experiments in the regions in which they overlap in p_r.

At larger neutron recoil angles of $\theta_{nq} \sim 75^o$ [Fig. 2(c)], the data follows the CD-Bonn PWIA (momentum distributions) up to p_r ∼100 MeV/c, and at $p_r \gtrsim$300 MeV/c, the FSIs become the dominat process and exhibit a smaller falloff with p_r which obscures any possibility of extracting the momentum distributions. This behaviour of FSI with larger recoil angles was predicted by the GEA[16**?**] and was verified in previous experiments[14, 17]. This experiment kinematics moves away from larger recoil angles and focuses on fowards angles at $\theta_{nq} \sim 40^o$ where the momentum distributions become accessible. As a result, our data at larger recoil angles is statistically limited.

For recoil angles at $\theta_{nq} = 35^o$ and 45^o shown in Figs. 2(a) and 2(b), all models predict similar behaviour of the momentum distribution for recoil momenta up to p_r ∼300 MeV/c which the data verifies. At larger p_r, however, the momentum distributions become increasingly sensitive to the different NN potentials, mainly a difference between the CD-Bonn and either the Paris or AV18 is observed.

In Fig. 2(a) for example, the data is clearly sensitive to the CD-Bonn momentum distributions between recoil momenta of $300 \lesssim p_r \lesssim 750$ MeV/c before transitioning to the Paris/AV18 potentials which is a behaviour that is not well described by any of the models. For recoil angles in Fig. 2(b), a similar behaviour can be observed, as the data is sensitive to the CD-Bonn momentum distributions but only up to $p_r \sim 580$ MeV/c as FSIs start

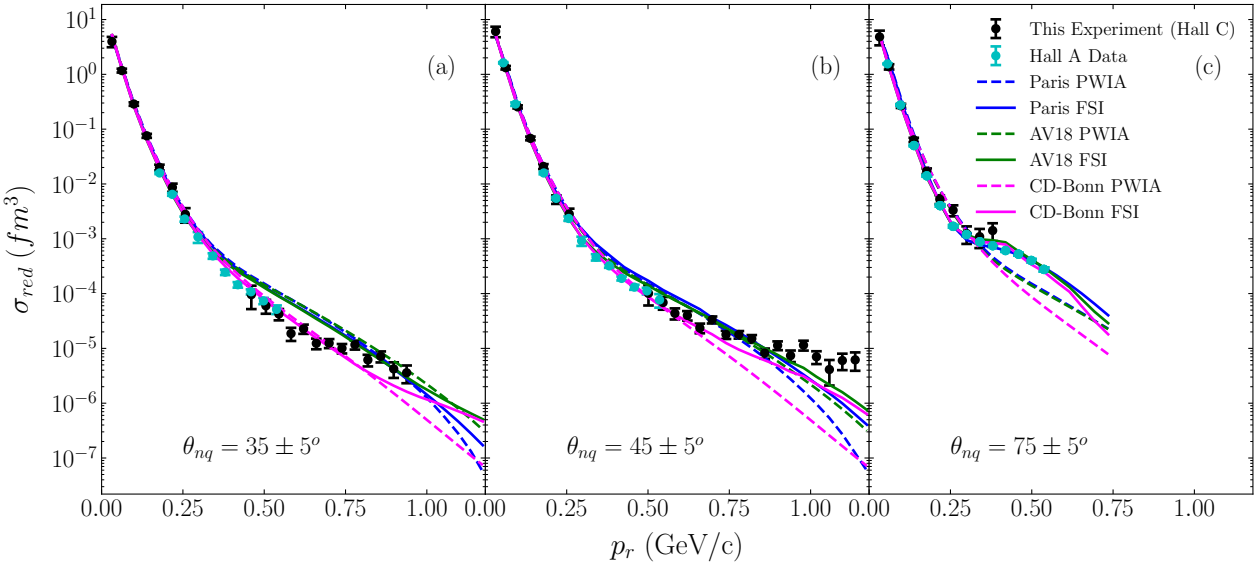

FIG. 2. The reduced cross section $\sigma_{red}(p_r)$ as a function of neutron recoil momentum p_r is shown in (a)-(c) for recoil angles $\theta_{nq} = 35^o, 45^o$ and 75^o, respectively, with a bin width of $\pm 5^o$. The data is compared to the previous Hall A experiment results as well as the Paris, AV18 and CD-Bonn theoretical reduced cross sections.

to dominate at lower p_r as opposed to Fig. 2(a). For $p_r > 580$ MeV/c, the data again exhibits a behaviour at the high momentum tails which either the CD-Bonn, Paris or AV18 potentials are unable to describe. In summary, this commissioning experiment extends the previous Hall A cross section measurements on the $^2H(e,e'p)n$ reaction to unprecedented large Q^2 and very high neutron recoil momenta at kinematics that enhances the high momentum components of the deuteron wavefunctions while suppressing long-range processes such as MECs or ICs. FSIs have also been largely suppressed by selecting a kinematic window found in the previous Hall A experiment where FSIs were found to be reduced and independent of missing momentum at recoil angles $35^o \leq \theta_{nq} \leq 45^o$. This experiment took advantage of that kinematic window and extended the cross section measurements beyond p_r ∼500 MeV/c. The experimental reduced cross sections were extracted and found to be best described by the CD-Bonn potential with sensitivity to the CD-Bonn momentum distributions up to $p_r \sim 580$ and 750 MeV/c for $\theta_{nq} \sim 45^o$ and 35^o, respectively before the data transitioning to other theoretical models, which is a behavior that was not predicted by any of the models. We conclude that these results although very interesting, does not have the sufficient statistics and the required number of high missing momentum settings to make a definitive argument about the underlying physics observed.

We acknowledge the outstanding support of the staff of the Accelerator and Physics Divisions at Jefferson Lab as well as the entire Hall C staff and technicians and all graduate students and users who took shifts or contributed to the equipment for the Hall C upgrade making all four commissioning experiments possible.

[1] K. S. Egiyan *et al.* (CLAS Collaboration), Observation of nuclear scaling in the $A(e,e')$ reaction at $x_B > 1$, Phys. Rev. C **68**, 014313 (2003).
[2] K. S. Egiyan *et al.* (CLAS Collaboration), Measurement of two- and three-nucleon short-range correlation probabilities in nuclei, Phys. Rev. Lett. **96**, 082501 (2006).
[3] R. Shneor *et al.* (Jefferson Lab Hall A Collaboration), Investigation of proton-proton short-range correlations via the $^{12}C(e,e'pp)$ reaction, Phys. Rev. Lett. **99**, 072501 (2007).
[4] N. Fomin, D. Higinbotham, M. Sargsian, and P. Solvignon, New results on short-range correlations in nuclei, Annual Review of Nuclear and Particle Science **67**, 129159 (2017).
[5] P. Ulmer *et al.*, Short-Distance Structure of the Deuteron and Reaction Dynamics in ^{2}H(e,e'p)n, https://www.jlab.org/exp_prog/proposals/01/PR01-020.pdf (2001), *Jefferson Lab Proposal E01-020*.
[6] C. Bochna *et al.*, Measurements of deuteron photodisintegration up to 4.0 gev, Phys. Rev. Lett. **81**, 4576 (1998).
[7] E. C. Schulte *et al.*, Measurement of the high energy two-body deuteron photodisintegration differential cross section, Phys. Rev. Lett. **87**, 102302 (2001).
[8] E. C. Schulte *et al.*, High energy angular distribution measurements of the exclusive deuteron photodisintegration reaction, Phys. Rev. C **66**, 042201 (2002).
[9] P. E. Ulmer *et al.*, ^{2}H$(e,e'p)n$ reaction at high recoil momenta, Phys. Rev. Lett. **89**, 062301 (2002).
[10] H. Arenhövel, W. Leidemann, and E. L. Tomusiak, Inclusive deuteron electrodisintegration with polarized electrons and a polarized target, Phys. Rev. C **43**, 1022 (1991).
[11] H. Arenhövel, W. Leidemann, and E. L. Tomusiak, Exclusive deuteron electrodisintegration with polarized electrons and a polarized target, Phys. Rev. C **46**, 455 (1992).
[12] H. Arenhövel, W. Leidemann, and E. L. Tomusiak, Nucleon polarization in exclusive deuteron electrodisintegration with polarized electrons and a polarized target, Phys. Rev. C **52**, 1232 (1995).
[13] H. Arenhövel, F. Ritz, H. Göller, and T. Wilbois, Consistent treatment of relativistic effects in electrodisintegration of the deuteron, Phys. Rev. C **55**, 2214 (1997).
[14] K. S. Egiyan *et al.* (CLAS Collaboration), Experimental study of exclusive ^{2}H$(e,e'p)n$ reaction mechanisms at high Q^2, Phys. Rev. Lett. **98**, 262502 (2007).
[15] M. M. Sargsian, Selected Topics in High Energy Semi-Exclusive Electro-Nuclear Reactions, International Journal of Modern Physics E **10**, 405457 (2001).
[16] L. L. Frankfurt, M. M. Sargsian, and M. I. Strikman, Feynman graphs and generalized eikonal approach to high energy knock-out processes, Phys. Rev. C **56**, 1124 (1997).
[17] W. U. Boeglin *et al.* (For the Hall A Collaboration), Probing the high momentum component of the deuteron at high Q^2, Phys. Rev. Lett. **107**, 262501 (2011).
[18] G. Niculescu, I. Niculescu, M. Burton, D. Coquelin, K. Nisson, and T. Jarell, Shms hodoscope scintillator detectors, https://hallcweb.jlab.org/document/howtos/shms_scintillator_hodoscope.pdf.
[19] M. Christy, P. Monaghan, N. Kalantarians, D. Biswas, and M. Long, Shms drift chambers, https://hallcweb.jlab.org/document/howtos/shms_drift_chambers.pdf.
[20] H. Mkrtchyan *et al.*, The lead-glass electromagnetic calorimeters for the magnetic spectrometers in hall c at jefferson lab, Nuclear Instruments and Methods in Physics Research Section A: Accelerators, Spectrometers, Detectors and Associated Equipment **719**, 85100 (2013).
[21] W. Li, *Heavy Gas Cherenkov Detector Construction for Hall C at Thomas Jefferson National Accelerator Facility*, Master's thesis, University of Regina (2012).
[22] D. Day, Preliminary design of the shms noble cerenkov detector, https://hallcweb.jlab.org/DocDB/0009/000933/001/shms-cerv6.pdf.
[23] C. Yero, Update on spectrometer offsets determination using h(e,e'p) elastics (2019), https://hallcweb.jlab.org/DocDB/0010/001036/002/HC_

SoftwareMeeting_Oct03_2019_pdf.pdf.
[24] C. Yero, Optics optimization for the d(e,e'p)n experiment [e12-10-003] (2019), https://hallcweb.jlab.org/DocDB/0010/001033/001/d2_optim.pdf.
[25] C. Yero, Proton absorption (2019), https://hallcweb.jlab.org/DocDB/0010/001020/002/ProtonAbsorption_slides.pdf.
[26] C. Yero, Hms target boiling studies (2019), https://hallcweb.jlab.org/DocDB/0010/001023/003/TargetBoiling_v2.pdf.
[27] P. E. Bosted, Empirical fit to the nucleon electromagnetic form factors, Phys. Rev. C **51**, 409 (1995).
[28] Conservative estimates on the systematic uncertainties of the total live and charge were made. Determination of systematics on these quantities is a work in progress. (Private communication with D. Mack).
[29] M. Lacombe, B. Loiseau, J. M. Richard, R. V. Mau, J. Côté, P. Pirès, and R. de Tourreil, Parametrization of the paris $n-n$ potential, Phys. Rev. C **21**, 861 (1980).
[30] T. D. Forest, Off-shell electron-nucleon cross sections: The impulse approximation, Nuclear Physics A **392**, 232 (1983).
[31] R. Machleidt, High-precision, charge-dependent bonn nucleon-nucleon potential, Phys. Rev. C **63**, 024001 (2001).
[32] R. B. Wiringa, V. G. J. Stoks, and R. Schiavilla, Accurate nucleon-nucleon potential with charge-independence breaking, Phys. Rev. C **51**, 38 (1995).

.